Journal of Solid State Chemistry **155,** 143–153 (2000)
doi:10.1006/jssc.2000.8915, available online at http://www.idealibrary.com on IDEAL®

New Inorganic–Organic Coordination Polymers Generated from Rigid or Flexible Bidentate Ligands and $Co(NCS)_2 \cdot xH_2O$

Yu-Bin Dong, Mark D. Smith, and Hans-Conrad zur Loye[1]

Department of Chemistry and Biochemistry, The University of South Carolina, Columbia, South Carolina 29208

Received June 15, 2000; in revised form July 31, 2000; accepted August 2, 2000

DEDICATED TO PROFESSOR J. M. HONIG

The coordination chemistry of the long rigid bidentate Schiff-base ligands 1,4-bis(3-pyridyl)-2,3-diaza-1,3-butadiene (L1), 2,5-bis(3-pyridyl)-3,4-diaza-2,4-hexadiene (L2), and of the flexible ligand 1,3-bis(4-pyridyl)propane with $Co(NCS)_2 \cdot xH_2O$ has been investigated. Three new coordination polymers were prepared and fully characterized by infrared spectroscopy, elemental analysis, thermogravimetric analysis, and single-crystal X-ray diffraction. The magnetic behavior of all compounds was also investigated and found to follow the Curie law. $[Co(NCS)_2(L1)_2 \cdot 2CH_2Cl_2]_n$ (1, monoclinic, $C2/m$; $a = 11.995(2)$ Å, $b = 14.596(3)$ Å, $c = 10.846(2)$ Å, $\beta = 110.99(3)^\circ$, $Z = 2$) features a two-dimensional non-interpenetrating distorted square pattern. $[Co(NCS)_2(L2)_2]_n$ (2, monoclinic, $P2_1/n$; $a = 9.5315(19)$ Å, $b = 17.299(4)$ Å, $c = 9.6646(19)$ Å, $\beta = 99.11(3)^\circ$, $Z = 2$) features a one-dimensional ring-like chain motif. Important C–H ⋯ S hydrogen bonding interactions exist in 2, which play a significant role in aligning the polymer strands in the crystalline solid. $[Co(1,3\text{-bis}(4\text{-pyridyl})propane)_2(NCS)_2 \cdot 0.33H_2O]_n$ (3, monoclinic, $P2_1/n$; $a = 18.701(4)$ Å, $b = 16.593(3)$ Å, $c = 20.696(4)$ Å, $\beta = 114.45(3)^\circ$, $Z = 4$) exhibits a polymeric pattern similar to that of 1. All three compounds feature similar $\{CoN_6\}$ pseudooctahedral coordination spheres. © 2000 Academic Press

Key Words: **coordination polymers; framework materials; hydrogen bonding; Schiff-base ligands.**

INTRODUCTION

Within the field of inorganic–organic coordination polymers, efforts to simultaneously utilize transition metal ions and organic spacers to form new extended framework structures have yielded diverse new materials (1–16), some of which have potential for applications such as catalysis, nonlinear optics, gas separation, magnetic devices, and molecular recognition (17–23). In the long run, research performed today may well enable us in the future to actually predict the topology and/or the connectivity of crystalline lattices based on the molecular structures of the small building blocks used in their assembly. This will, ideally, lead to the rational design of framework materials for specific applications. Currently, the most efficient approach to preparing framework materials is via direct chemical combination of functional inorganic and organic components, a method which has proven quite fruitful (1–16).

Several rigid bidentate N-donor ligands, such as 4,4′-bipyridine, 1,2-bis(4-pyridyl)ethene, 1,2-bis(4-pyridyl) ethyne, as well as flexible N-donor ligands like 1,2-bis(4-pyridyl)ethane and 1,3-bis(4-pyridyl)propane ("4,4′-trimethylenedipyridine"), have been utilized by us (24–29) and numerous other research groups (1–3) to construct novel coordination polymers. These ligands, shown in Fig. 1, are an important class of organic ligands for the design and synthesis of new framework materials, often having unusual structures. However, the above-mentioned ligands do not contain free, active, polar organic functional groups such as –C ≡ N, –CR=N–, –COOH, –CHO, –OH, which are believed to play a central role in the construction of molecule-based functional materials (30, 31). Recently, we designed and synthesized two new long, conjugated Schiff-base ligands, namely, 1,4-bis(3-pyridyl)-2,3-diaza-1,3-butadiene (L1) and 2,5-bis(3-pyridyl)-3,4-diaza-2,4-hexadiene (L2) (28, 29). The structures of these ligands, including the relative orientations of the terminal nitrogen donors and the zig-zag conformation of the spacer moiety (–CR=N–N=CR–, R=H, $-CH_3$) between the two pyridyl groups (Fig. 1), might lead to the formation of coordination polymers with network patterns not achievable by other common rigid linking ligands (4,4′-bipyridine, etc.). Moreover, the nitrogen atoms in the –CR=N–N=CR– functional group in these ligands can potentially form hydrogen bonds (acting as the acceptors) with donor groups to generate supramolecular systems with interesting host–guest chemistry (28). Herein, we wish to report three new coordination polymers, namely $Co(L1)_2(NCS)_2 \cdot 2CH_2Cl_2$ (**1**), $Co(L2)_2(NCS)_2$ (**2**), and $Co(1,3\text{-bis}(4\text{-pyridyl})propane)_2(NCS)_2 \cdot 0.33H_2O$ (**3**), generated from the reaction between the new rigid Schiff-base

[1] To whom correspondence should be addressed. E-mail: zurloye@sc.edu.

0022-4596/00 $35.00

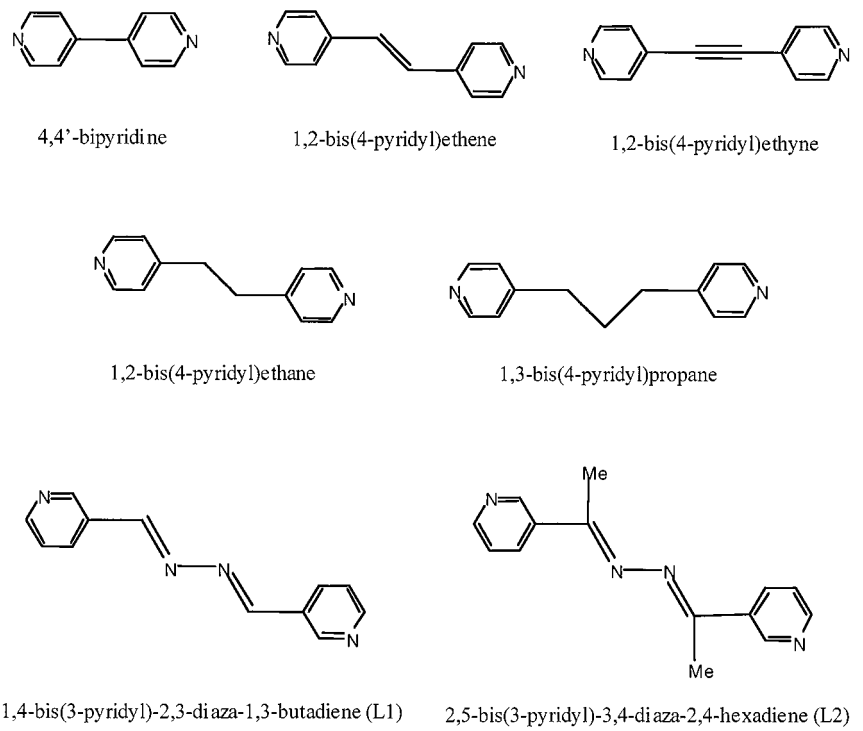

FIG. 1. Rigid and flexible organic bipyridyl-based ligands used in the construction of coordination polymer frameworks.

ligands L1, L2, the long flexible ligand 1,3-bis(4-pyridyl) propane, and $Co(NCS)_2 \cdot xH_2O$ in a CH_2Cl_2–MeOH mixed solvent system. In this paper we again demonstrate the successful use of these new Schiff-base ligands to link metal centers and to generate new coordination polymers with novel structures. Moreover, we have confirmed that the –CH=N–N=CH– spacer in L1 can indeed act as a hydrogen bond acceptor, aiding it in binding organic guest molecules within framework cavities.

EXPERIMENTAL

Materials and Methods

$Co(NCS)_2 \cdot xH_2O$ and 1,3-bis(4-pyridyl)propane were purchased from Aldrich and used without further purification. The syntheses of L1 and L2 will be published elsewhere (28, 29). IR spectra were recorded on a Perkin-Elmer 1600 FTIR spectrometer as KBr pellets in the 4000–400 cm^{-1} range. Thermogravimetric analysis (TGA) was carried out on a TA Instruments SDT 2960 simultaneous DTA-TGA in a helium atmosphere using a heating rate of 10°C/min. Compounds **1–3** were heated from 20 to 600°C. The magnetic susceptibilities of **1–3** were measured as a function of temperature using a Quantum Design MPMS XL SQUID magnetometer in an applied field of 5 kOe. Clear gelatin capsules were used as sample containers. Elemental analysis was performed by National Chemical Consulting.

Synthesis of $Co(NCS)_2$(1,4-*bis*(3-*pyridyl*)-2,3-*diaza*-1,3-*butadiene*)$_2 \cdot 2CH_2Cl_2$ (**1**). A methylene chloride solution (7 mL) of 1,4-bis(3-pyridyl)-2,3-diaza-1,3-butadiene (126 mg, 0.66 mmol) was allowed to diffuse into a methanol solution (8 mL) of $Co(NCS)_2 \cdot xH_2O$ (53 mg, 0.30 mmol) in a test tube for 1 week. Large orange crystals formed at the methylene chloride/methanol interface. Crystals were collected by filtration and washed several times with *n*-hexane (yield 75%, based on $Co(NCS)_2 \cdot xH_2O$). IR (KBr, cm^{-1}): 2072.5 (s), 1692.1 (w), 1631.8 (s), 1548.4 (w), 1530.2 (w), 1483.4 (s), 1413.3 (s), 1383.2 (s), 1322.2 (s), 1190.1 (s), 1021.9 (s), 881.9 (s), 696.0 (s), 641.7 (s), 481.5 (m), 453.8 (m), 402.7 (m). Anal. Calcd. for $CoC_{28}H_{26}Cl_4N_{10}S_2$: C, 43.78; H, 3.39; N, 18.24%. Found: C, 43.55; H, 3.38; N, 17.98%.

Synthesis of $Co(NCS)_2$(2,5-*bis*(3-*pyridyl*)-3,4-*diaza*-2,4-*hexadiene*)$_2$ (**2**). The procedure is similar to that described for the preparation of compound **1**, except 2,5-bis(3-pyridyl)-3,4-diaza-2,4-hexadiene (0.66 mmol) was used instead of 1,4-bis(3-pyridyl)-2,3-diaza-1,3-butadiene. Yield of red crystals, 72% (based on $Co(NCS)_2 \cdot xH_2O$). IR (KBr, cm^{-1}): 2052.7 (s), 1692.5 (w), 1613.2 (s), 1484.0 (s), 1414.7 (s), 1307.5 (s), 1196.9 (s), 1089.4 (s), 1043.5 (s), 819.9 (s), 781.6 (s), 702.9 (s), 643.6 (s), 573.1 (w), 483.1 (m), 428.4 (m), 414.9 (s). Anal. Calcd. for $CoC_{30}H_{28}N_{10}S_2$: C, 55.24; H, 4.30; N, 21.48%. Found: C, 55.34; H, 4.22; N, 21.20%.

Synthesis of $Co(SCN)_2$(1,3-*bis*(4-*pyridyl*)*propane*)$_2$ (**3**). Compound **3** was obtained upon carefully layering a

solution of $Co(NCS)_2 \cdot xH_2O$ (60 mg, 0.34 mmol) in methanol (8 mL) onto a solution of 4,4′-trimethylenebipyridine (131 mg, 0.66 mmol) in methylene chloride (8 mL). Large red-orange crystals formed at the methanol/methylene chloride interface in about 2 weeks, and were collected by filtration in 75% yield (based on $Co(NCS)_2 \cdot xH_2O$). IR (KBr, cm^{-1}): 2943.8(s), 2854.8(m), 2054.0(s), 1613.7(s), 1557.7(s), 1500.4(s), 1422.7(s), 1352.1(w), 1223.0(s), 1069.6(s), 1017.1(s), 964.9(w), 853.1(m), 841.6(w), 808.0(s), 762.7(m), 732.6(w), 612.1(m). Anal. Calcd. for $Co_2C_{56}H_{56.66}N_{12}O_{0.33}S_4$: C, 58.51; H, 4.93; N, 14.63%. Found: C, 58.32; H, 4.90; N, 14.20%.

Single-crystal structure determination. Single crystals of **1–3** suitable for diffraction studies were selected and epoxied in air onto thin glass fibers. Intensity measurements were made at 21°C using a Rigaku AFC6S four-circle diffractometer equipped with Mo$K\alpha$ radiation ($\lambda = 0.71069$ Å). For each compound, the initial unit cell was determined from 15 reflections randomly located using the AFC6 automatic search, center, index, and least-squares routines. After data collection, each cell was refined using 25 high-angle reflections in the range $35° < 2\theta < 2\theta_{max}$. Three standard reflections measured every 150 reflections showed no significant decay during data collection for each crystal. All structures were solved and refined by a combination of direct methods and difference Fourier syntheses, using SHELXTL (32). After locating and refining all nonhydrogen atoms with isotropic thermal parameters, an absorption correction (DIFABS) (33) was applied. Subsequently, all nonhydrogen atoms were refined with anisotropic displacement parameters. Hydrogen atoms were placed in the calculated positions and refined using a riding model. Crystal data, data collection parameters, and refinement statistics for **1–3** are listed in Table 1. Important interatomic bond distances and bond angles for **1–3** are given in Tables 2–4.

RESULTS AND DISCUSSION

Synthesis

The coordination polymers **1–3** are readily synthesized by solution reactions between the new ligands 1,4-bis(3-pyridyl)-2,3-diaza-1,3-butadiene (L1), 2,5-bis(3-pyridyl)-3,4-diaza-2,4-hexadiene (L2), and the flexible ligand 1,3-bis(4-pyridyl)propane with $Co(NCS)_2 \cdot xH_2O$. When a solution of L1, L2, or 1,3-bis(4-pyridyl)propane in methylene chloride was treated with $Co(NCS)_2 \cdot xH_2O$ in methanol in a molar ratio of 1:2 (metal-to-ligand), compounds **1–3**, respectively, were obtained as polymeric materials. Compounds **1** and **3** feature two-dimensional nets, while compound **2** adopts a one-dimensional chain pattern. Single crystals of compound **3** can also be grown out of other solvent combinations, such as CH_3COCH_3/H_2O, THF/CH_3CN, or CH_2Cl_2/CH_3CN. The crystals are identical to those grown out of the CH_2Cl_2/MeOH mixture, as confirmed by X-ray powder diffraction. We were not able to

TABLE 1
Crystallographic Data for 1–3

Formula:	$CoC_{28}H_{26}N_{10}S_2Cl_4$ **1**	$CoC_{30}H_{28}N_{10}S_2$ **2**	$Co_2C_{56}H_{56.66}N_{12}O_{0.33}S_4$ **3**
Formula weight	767.44	568.49	543.69
Crystal system	Monoclinic	Monoclinic	Monoclinic
Space group	$C2/m$	$P2_1/n$	$P2_1/n$
a (Å)	11.995(2)	9.5315(19)	18.701(4)
b (Å)	14.596(3)	17.299(4)	16.593(3)
c (Å)	10.846(6)	9.6646(19)	20.696(4)
α (°)	90	90	90
β (°)	110.99(3)	99.11(3)	114.65(3)
γ (°)	90	90	90
V (Å^3)	1772.6(6)	1573.4(5)	5846(2)
Z	2	2	4
ρ calc. (g/cm^3)	1.438	1.376	1.305
μ (Mo$K\alpha$) (cm^{-1})	9.532	7.353	5.385
Temperature (°C)	21	21	21
No. of reflections ($I > 3\sigma$)	1648	2463	10326
Residuals[a]			
$R1$; $wR2$ (all data)	0.068; 0.176	0.048; 0.086	0.064; 0.130
Goodness-of-fit	1.056	1.093	1.010

[a] $R1 = \sum||F_o| - |F_c||/\sum|F_o|$. $wR2 = \{\sum[w(F_o^2 - F_c^2)^2]/\sum[w(F_o^2)^2]\}^{1/2}$; $GOF = \{\sum[w(F_o^2 - F_c^2)^2]/(n-p)\}^{1/2}$ (n = No. of reflections; p = No. of refined parameters). $w = 1/[\sigma^2(F_o^2) + (aP)^2 + bP]$, where P is $[2F_c^2 + \max(F_o^2, 0)]/3$.

TABLE 2
Interatomic Distances (Å) and Bond Angles (°) with ESDs ( ) for 1

Co–N(1)	2.221(3)	Co–N(3)	2.091(4)
S–C(7)	1.613(5)	N(3)–C(7)	1.159(7)
C(1)–N(1)	1.346(5)	C(1)–C(2)	1.370(6)
N(3)–Co–N(3)[a]	180	N(1)–Co–N(3)	90.03(11)
N(1)–Co–N(1)[a]	180	N(3)–C(7)–S	178.5(5)
C(7)–N(3)–Co	171.9(4)		

[a] Symmetry equivalent atoms.

TABLE 4
Interatomic Distances (Å) and Bond Angles (°) with ESDs ( ) for 3

Co(1)–N(6)	2.093(5)	Co(1)–N(5)	2.116(5)
Co(1)–N(4)	2.166(4)	Co(1)–N(2)	2.166(4)
Co(1)–N(3)	2.189(4)	Co(1)–N(1)	2.201(4)
S(1)–C(27)	1.622(6)	S(1)–C(28)	1.630(6)
N(1)–C(5)	1.327(5)	C(1)–C(2)	1.372(7)
N(6)–Co(1)–N(5)	177.59(16)	N(6)–Co(1)–N(2)	90.71(16)
N(4)–Co(1)–N(2)	177.87(16)	N(6)–Co(1)–N(1)	89.94(16)
N(3)–Co(1)–N(1)	175.70(14)	N(2)–Co(1)–N(1)	94.47(14)

[a] Symmetry equivalent atoms.

grow single crystals of compounds **1** and **2** suitable for X-ray diffraction from other mixed solvent systems (e.g., CH_3COCH_3/H_2O, THF/CH_3CN, CH_2Cl_2/CH_3CN). Toluene and 1,4-dioxane were also tried, however, again only poor quality crystals were obtained. Compounds **1–3** are air-stable and are insoluble in water and common organic solvents.

Structures

Compound 1. Single crystal X-ray analysis reveals that, as shown in Fig. 2, each Co(II) center sits on a 2/*m* symmetry site, with the crystallographic mirror plane passing through two NCS^- counterions. The coordination sphere of each Co(II) metal center is defined by four nitrogen donors from four equivalent bridging L1 ligands (N(1)–Co = 2.221(3) Å (×4)) and two nitrogen donors from two N-coordinated coordinated NCS^- counterions (N(3)–Co = 2.091(4) (×2)). The sulfur atoms remain uncoordinated. The coordination geometry can be described as an equatorial plane consisting of four N(1) nitrogen donors, with the axial positions occupied by two N(3) nitrogen donors. The Co–N(1) (L1) and Co–N(3) (NCS^-) bond distances are quite similar to corresponding distances in $Co(NCS)_2(pyrazine)_2$ and $Co(NCS)_2(4,4'\text{-bipyridine})_2 \cdot 2(CH_3CH_2)_2O$ (34) and in $Co(NCS)_2(pyrimidine)_2$ (35). The NCS^- group is almost linear with a N–C–S angle of 178.5(5)°. It is worth pointing out that the connection between the Co(II) center and the NCS^- counterion is also linear, with a Co–N(3)–C(7) angle of 171.9(4)°. This angle is noticeably larger than that found in the related compounds $Co(NCS)_2(pyrazine)_2$ (158.8(3)°), and $Co(NCS)_2(4,4'\text{-bipyridine})_2 \cdot 2(CH_3CH_2)_2O$ (153.2(3)°) (34). The four long L1 ligands do not lie in the $[CoN_4]$ plane but are located above and below the plane to produce an "X-shaped" building block (Fig. 2). The two 3-pyridyl rings in each L1 ligand are coplanar.

In the solid state, the "X-shaped" building blocks connect to each other to generate a novel two-dimensional, noninterpenetrating distorted square framework, shown in Fig. 3. Each square unit consists of four Co(II) atoms and four L1 ligands, which form a 44-membered ring structure (Fig. 3a). The Co ··· Co contact in each distorted square is 12.66(3) Å and the effective (crystallographic) cross section is ca. 12.66 × 12.66 Å (36). This cross section is significantly larger than that in related compounds generated from 4,4′-bipyridine and transition metals (Zn, Ni, Cu, Cd), which crystallize with a similar square pattern (crystallographic dimensions ca. 8 × 8 Å) (17, 37–39). There are two sets of

TABLE 3
Interatomic Distances (Å) and Bond Angles (°) with ESDs ( ) for 2

Co–N(1)	2.225(3)	Co–N(5)	2.071(3)
Co–N(4)	2.221(3)	S–C(15)	1.616(4)
C(15)–N(5)	1.156(5)	C(8)–N(3)	1.280(5)
N(5)–Co–N(5)[a]	180	N(5)–Co–N(1)	89.76(13)
N(1)–Co–N(1)[a]	180	N(4)[a]–Co–N(1)	92.39(12)
N(5)–C(15)–S	179.0(4)	C(15)–N(5)–Co	170.1(3)

[a] Symmetry equivalent atoms.

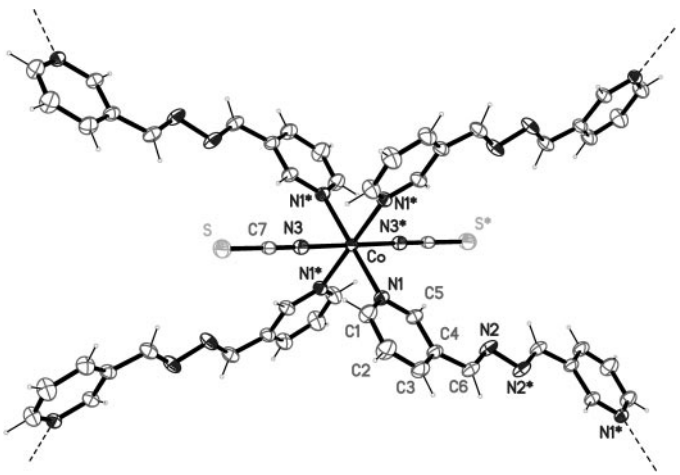

FIG. 2. ORTEP drawing of **1**, showing the coordination of cobalt. Ellipsoids are shown at the 30% probability level.

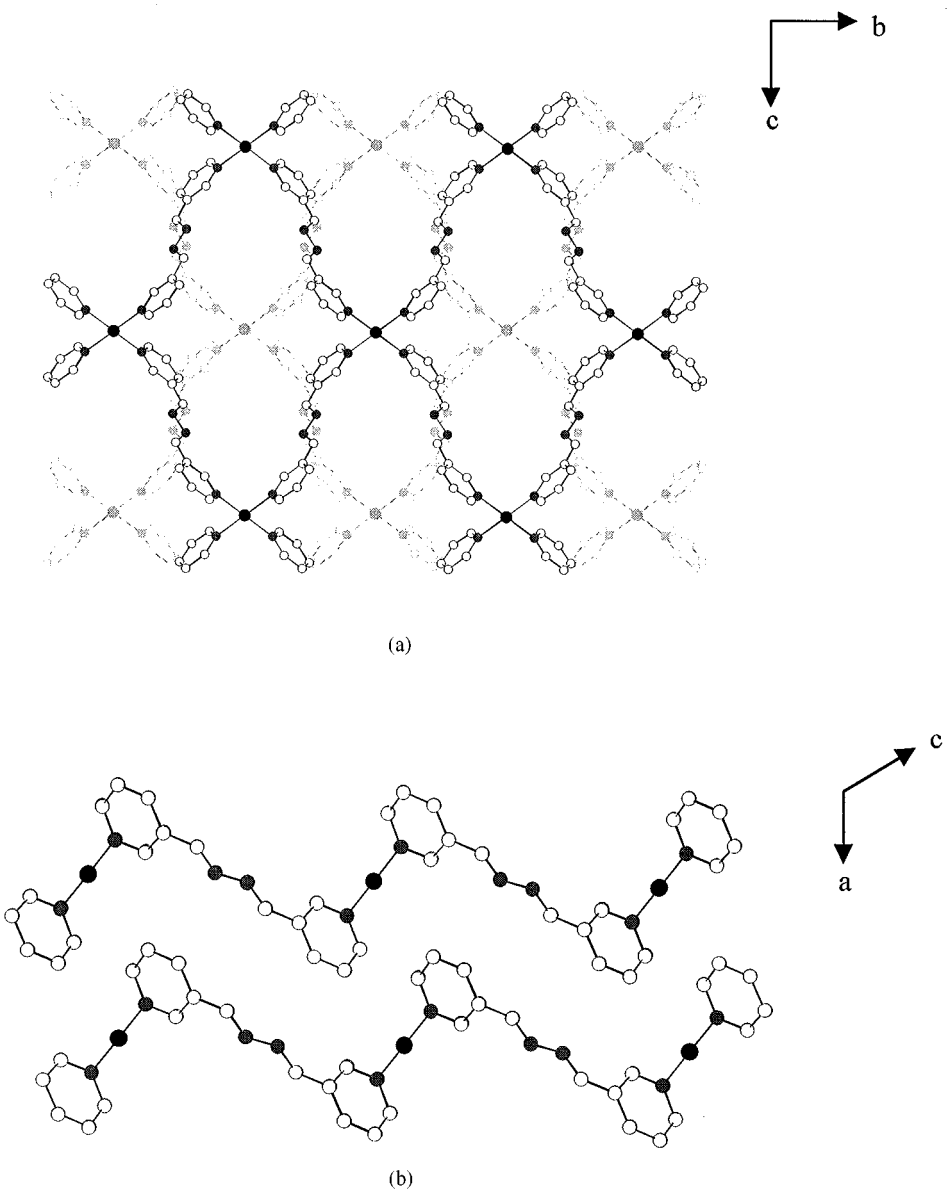

FIG. 3. (a) Two-dimensional non-interpenetrating distorted square network in **1** (viewed down the crystallographic *a*-axis). One framework set is highlighted. (b) Non-interpenetrating stacking of networks in **1**. Co(II) centers are shown as black circles, carbon atoms as open circles. Nitrogen atoms are shown as gray circles. NCS^- counterions and hydrogen atoms are omitted for clarity.

equivalent two-dimensional nets in **1**, which stack together in an "…ABAB…" fashion down the crystallographic *a* axis, such that the Co(II) centers in one net occupy the center of the channels formed by the other (Fig. 3a). The closest Co ⋯ Co contact between the two adjacent layers is 9.45(4) Å. A view of how these undulating layers stack upon one another is given in Fig. 3b. Although this stacking arrangement effectively reduces the void volume present in the structure, considerably large distorted square channels running along the [101] crystallographic direction still remain. These channels, shown in Fig. 4, have crystallographic dimensions of 9.45×9.45 Å (36), in which disordered CH_2Cl_2 guest molecules are located. There are two crystallographically independent CH_2Cl_2 molecules per metal atom, which are all oriented so that they are weakly hydrogen bonded to the nonterminal nitrogen atoms (N(2)) in the –CH=N–N=CH– linkages of the L1 ligands (N(2) ⋯ H(9A) = 2.62(3) Å, N(2) ⋯ C(9) = 3.53(4) Å, and N(2) ⋯ H(9A)–C(9) = 156.22(4)°) (28, 40). These C–H ⋯ N hydrogen bonding interactions described here, though weak, have an important influence on both the clathration ability and stability of **1**. The capability of **1** to engage in hydrogen

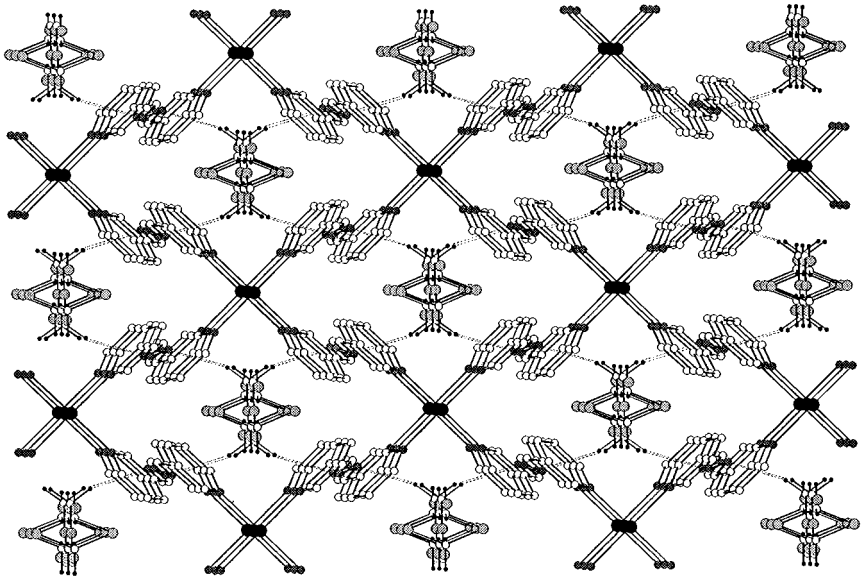

FIG. 4. View down the channels in **1**, in which CH_2Cl_2 guest molecules are located. Co(II) centers are shown as black circles, carbon atoms as open circles. Chlorine and nitrogen atoms are shown as large and small gray circles, respectively. NCS^- counterions and hydrogen atoms on L1 ligands are omitted for clarity. C–H ··· N hydrogen bonds are shown as dotted lines.

bonding with solvent molecules via the inner nitrogen atoms in the ligand L1 is a possible explanation for the relative stability of **1** compared to $Co(NCS)_2$(4,4′-bipyridine)$_2 \cdot 2(CH_3CH_2)_2O$ (34) and $Co(NO_3)_2$(1,2-bis(4-pyridyl)ethene)$_{1.5} \cdot 3CHCl_3$ (41), both of which lose their guest molecules immediately upon removal from the mother liquor. In the latter compounds, there are no stabilizing interactions between the organic guest molecules and the host framework structure, due to the absence of hydrogen bonding acceptors on the linking ligands.

Compound 2. The coordination environment of Co(II) in **2** is similar to that found in **1**. As shown in Fig. 5, each Co(II) center adopts a slightly distorted octahedral $\{CoN_6\}$ coordination geometry, with the equatorial plane defined by four pyridyl nitrogen donors from four crystallographically equivalent L2 ligands; the axial positions are occupied by

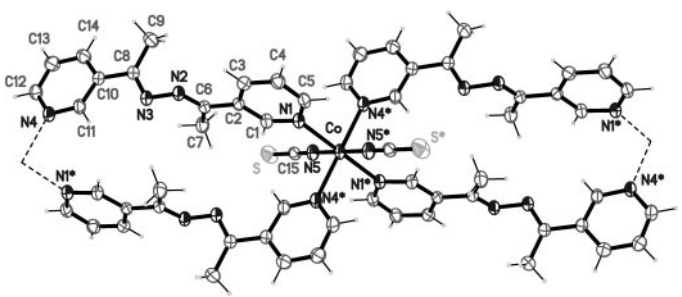

FIG. 5. ORTEP drawing of the coordination environment of cobalt in **2**. Ellipsoids are shown at the 30% probability level.

two nitrogen atoms from two crystallographically equivalent NCS^- counterions. The Co–N (L2) bond lengths are 2.221(3) and 2.225(3) Å, respectively, which are comparable to the corresponding bond distances in **1**. The Co–N (NCS^-) bond distance is 2.071(3) Å, which is slightly shorter than that found in **1**. The NCS^- group is nearly linear with a N–C–S angle of 179.0(4)°. In contrast to the L1 ligand, the two 3-pyridyl rings in each L2 ligand are no longer coplanar. The dihedral angle between the terminal pyridyl groups is 90°, which, presumably, is due to the steric congestion of the two methyl groups. The two methyl groups are located in the α positions relative to the two C=N groups and the contacts between the methyl carbons (C(7) and C(9)) and the nitrogens (N(2) and N(3)) in the $-C(CH_3)=N-N=C(CH_3)-$ spacer are quite close ($N(2) \cdots C(7) = N(3) \cdots C(9) = 2.44(3)$ and $N(2) \cdots C(9) = N(3) \cdots C(7) = 2.75(4)$ Å), suggesting that the uncoordinated nitrogen atoms interact with methyl carbon atoms by weak electrostatic forces (26). Consequently, the two methyl groups in each L2 ligand should be weakly acidic. As shown in Fig. 5, the orientation of the terminal nitrogen donors on the 3-pyridyl rings are different from those in **1**, in spite of the fact that the building block of **2** also exhibits a "X-shaped" arrangement.

In the solid state, as shown in Fig. 6, compound **2** adopts a one-dimensional chain motif, with the Co(II) centers linked together via the four crystallographically equivalent L2 ligands. This results in an undulating, one-dimensional chain running along the crystallographic [101] direction. The individual "links" in the chains consist of $Co_2(L2)_2$ units, which can be viewed as 22-membered rings enclosed

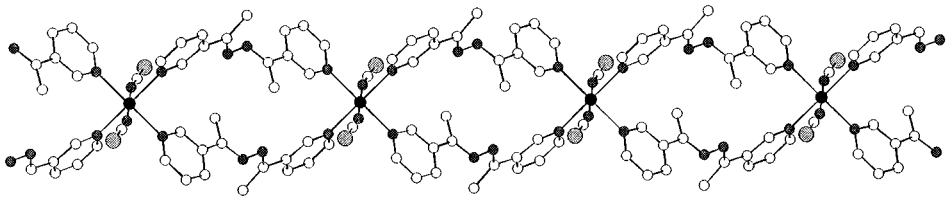

FIG. 6. One-dimensional chain structure of **2**. Co(II) centers are shown as black circles, carbon atoms as open circles. Sulfur and nitrogen atoms are shown as large and small gray circles, respectively. Hydrogen atoms are omitted for clarity.

by two Co(II) atoms and two L2 ligands. The approximate dimensions of the rings are 12×5 Å (36). The intrachain Co $\cdots$ Co separation is 12.45(4) Å. The NCS^- ions are located on both sides of the $Co_2(L2)_2$ ring planes. Interestingly, there are two sets of one-dimensional $Co_2(L2)_2$ chains in **2**. Each set stacks together in a face-to-face fashion to

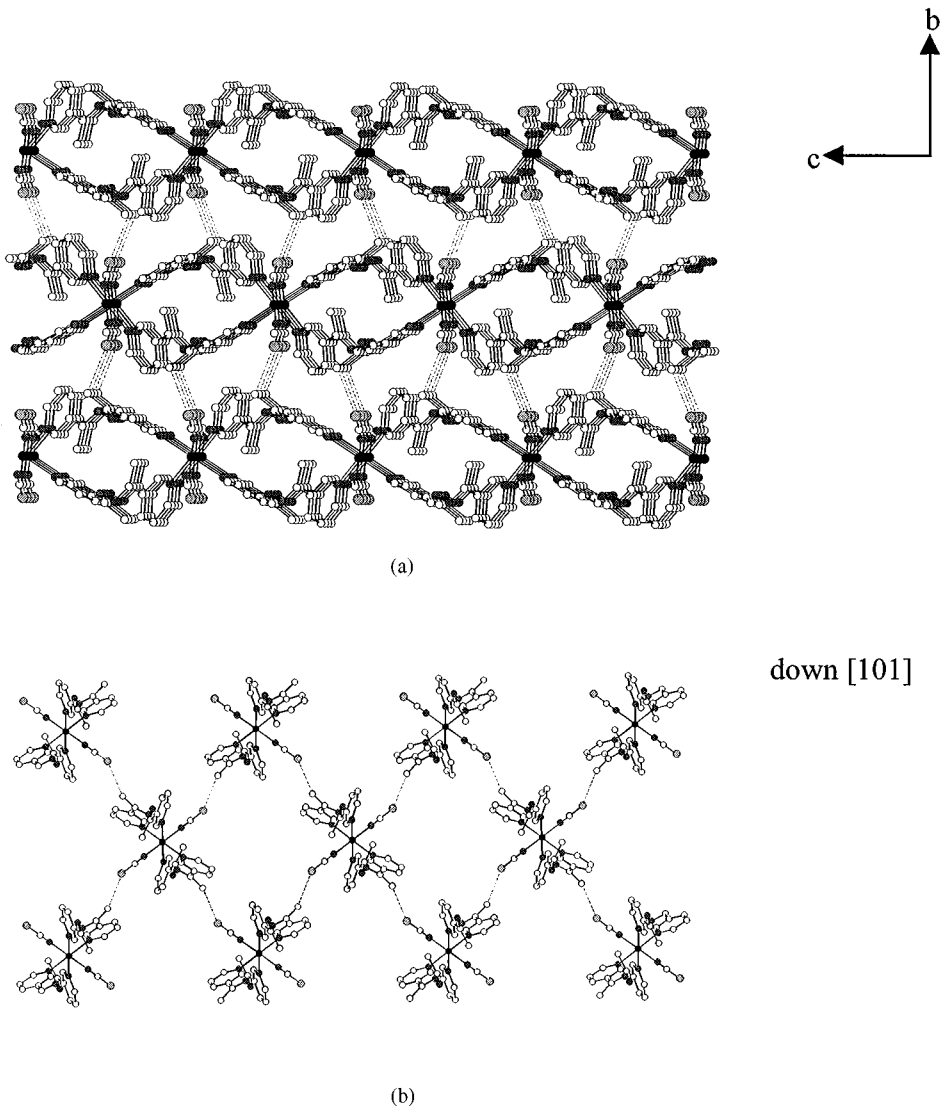

FIG. 7. (a) Three-dimensional hydrogen-bonded network of linked 1D chains, viewed down the crystallographic *a*-axis. (b) View down the crystallographic [101] (chain) direction. Co(II) centers are shown as black circles, carbon atoms as open circles. Sulfur and nitrogen atoms are shown as large and small gray circles, respectively. Hydrogen atoms are omitted for clarity. C–H $\cdots$ S hydrogen bonds are shown as dotted lines.

generate elliptical channels along the crystallographic [101] direction, shown in Fig. 7a. The interchain Co ··· Co contact is 9.531(4) Å. In addition, these two sets of one-dimensional chains are linked together by weak interchain C–H ··· S hydrogen bonding interactions into a three-dimensional network (Fig. 7b). The C–H ··· S hydrogen bond involves the uncoordinated S atoms of the monodentate NCS^- and H(9C) on the weakly acidic methyl group of an L2 ligand in an adjacent chain. The S ··· H(9C) contact is 2.831(4) Å. The S ··· C(9) distance and S ··· H(9C)–C(9) angle are 3.719(4) Å and 154.25(13)°, respectively. The existence and structural importance of weak C–H ··· *X* (*X* = heteroatom) hydrogen bonding interactions are now well established (40) and are present in many molecular and polymeric compounds. The C–H ··· S hydrogen bonding interaction is especially attractive because it has been proven to be a very important factor in the formation of organic conducting and superconducting compounds (42). The S ··· H–C hydrogen bonds described here, although weak, contribute significantly to the structural organization of **2** in the crystalline phase. The structure of **2** and of $Fe(NCS)_2$(1,2-bis(4-pyridyl)ethane)$_2$ (43) are related. Both structures contain one-dimensional chains consisting of $M_2(L)_2$ rings. In the Fe(II) compound, the intrachain Fe ··· Fe distance is 9.995(3) Å, which is remarkably shorter than the intrachain Co ··· Co contact in **2** (12.45(4) Å). The Fe ··· Fe interchain distance (10.768(4) Å), however, is longer than the interchain Co ··· Co contact in **2**. In addition, C–H ··· S hydrogen bonding interactions are also found in the Fe compound, where they serve as links to connect $Fe(NCS)_2$(1,2-bis(4-pyridyl)ethane)$_2$ one-dimensional chains into a two-dimensional network.

Varying the *R* group (from H in L1 to CH_3 in L2) on the –C*R*=N–N=C*R*– spacer, is, for the same solvent system and metal-to-ligand ratio (1:2), a decisive factor in determining the orientation of the nitrogen donors on the terminal pyridyl groups, and, moreover, the topologies of the polymeric products.

Compound 3. In order to further investigate the functionality of bidentate pyridyl-containing ligands, the flexible ligand 1,3-bis(4-pyridyl)propane (also known as 4,4′-trimethylenedipyridine) was reacted with $Co(NCS)_2 \cdot xH_2O$ using analogous reaction conditions as with the rigid bidentate ligands L1 and L2. The structure of the resulting compound **3** is similar to that of **1**. The flexible 1,3-bis(4-pyridyl)propane ligands bridge Co(II) centers, and the NCS^- counterion serves as an N-bound terminal ligand. Figure 8 shows the local coordination of the Co(II) center. There are two crystallographically independent Co(II) centers (Co(1) and Co(2)) in **3**. Only the coordination environment of Co(1) is shown in Fig. 8 and discussed here, because the structural features of the two independent coordination spheres and resulting polymeric networks are essentially the same

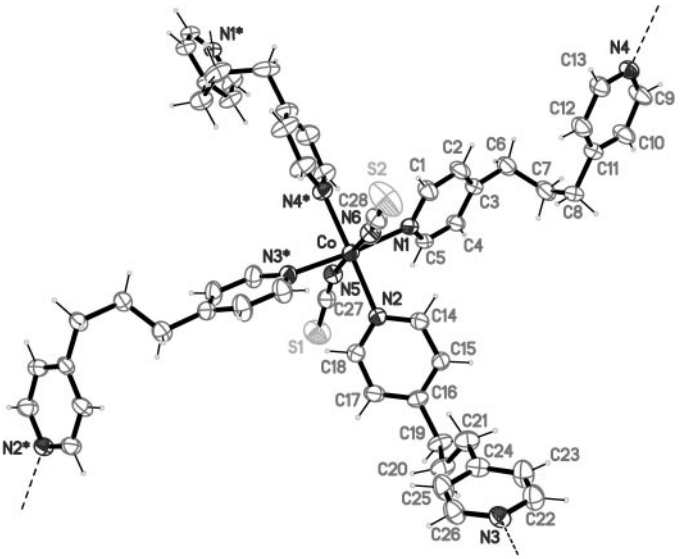

FIG. 8. ORTEP drawing of the coordination environment at the cobalt atoms in **3**. Ellipsoids are shown at the 30% probability level.

(Table 4 includes only selected bond lengths and bond angles for Co(1)). In harmony with compounds **1** and **2**, Co(1) also features a $\{CoN_6\}$ distorted octahedral coordination sphere defined by nitrogen donors from four 1,3-bis(4-pyridyl)propane ligands and from two monodentate NCS^- groups. The Co–N (1,3-bis(4-pyridyl)propane) bond lengths range from 2.116(4) to 2.201(4) Å, which are slightly shorter than those in **1** and **2**. The Co–N (NCS^-) bond distance is 2.093(5) Å, which is almost identical with those in **1** and **2**. Two terminal NCS^- groups are again close to linear, with N–C–S angles of 179.2(6) and 178.9(6)°, respectively.

The polymeric motif in compound **3** is quite similar to that in **1**. Two crystallographically independent Co(II) centers (Co(1) and Co(2)) are bridged by 1,3-bis(4-pyridyl) propane ligands, respectively, into two sets of undulating two-dimensional nets with a distorted square motif involving a 48-membered ring structure. In **3**, though, the two sets of two-dimensional sheets interlock each other in the same plane (the crystallographic *ab* plane) to generate a twofold interpenetrating network (Figs. 9a and 9b), in which two sets of Co(1,3-bis(4-pyridyl)propane) layers are staggered relative to each other (Fig. 9a). The Co ··· Co contacts in each distorted square unit are 12.23(4) and 12.78(4) Å, comparable to the corresponding distances in **1**. These interpenetrated pairs of networks stack upon one another along the *c*-axis, generating a three-dimensional layered structure. The combination of interpenetration and efficient layer stacking effectively eliminates the void space accessible to solvents, and indeed only a small amount of water (0.33 molecules per formula) is present between the layers.

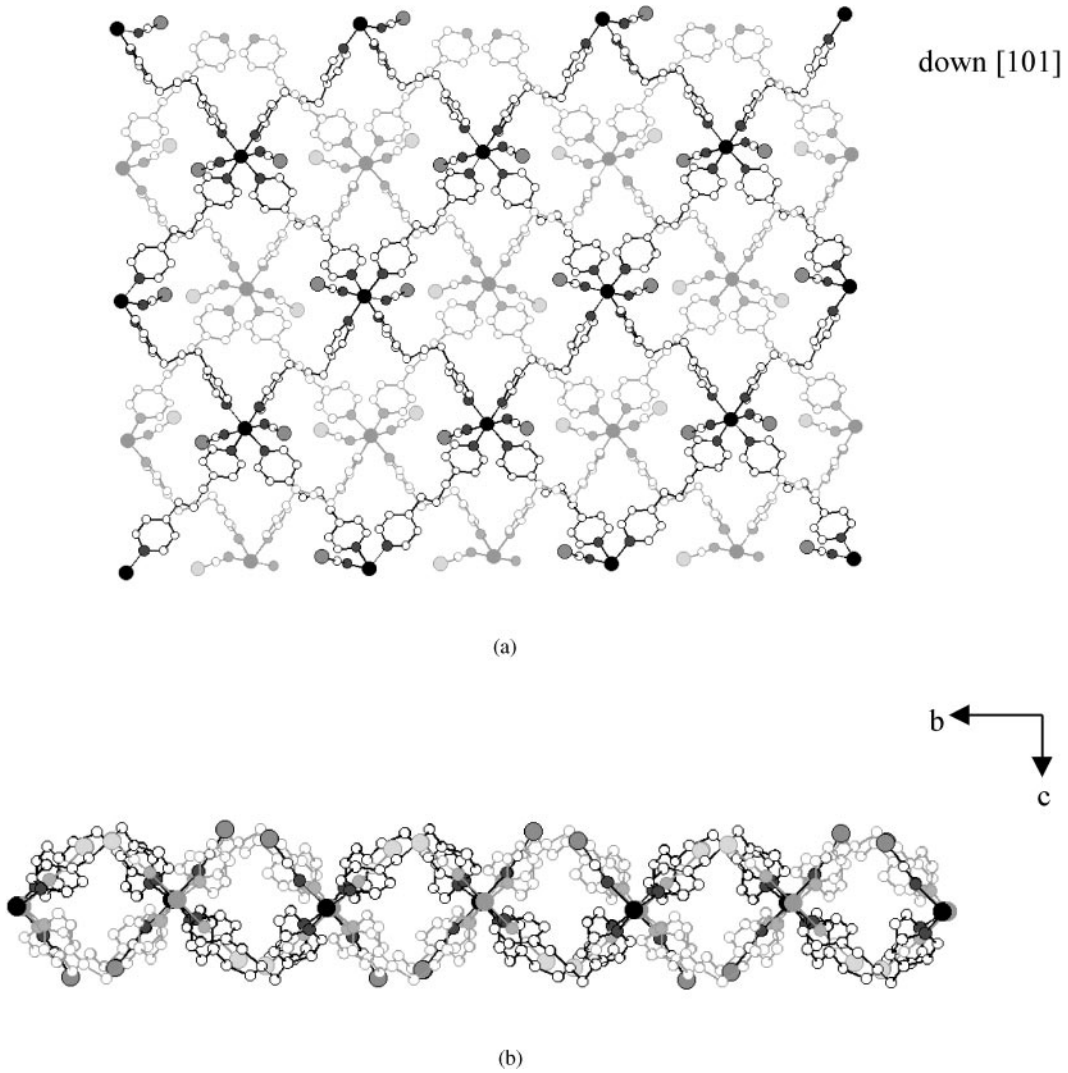

FIG. 9. (a) Two-dimensional interpenetrating distorted square network in **1** viewed down the crystallographic [101] direction. (b) View down the *a*-axis. One set of frameworks is highlighted. Co(II) centers are shown as black circles, carbon atoms as open circles. Nitrogen atoms are shown as gray circles. Hydrogen atoms are omitted for clarity.

Thermogravimetric analyses. Thermogravimetric analyses were carried out using a TA Instrument SDT 2960 simultaneous DTA-TGA under flowing helium at a heating rate of 10°C/min. Compounds **1–3** were heated from 30 to 600°C. TGA showed that **1** is stable up to 200°C, with the first weight loss of 22.1% from occurring in the range 200–256°C, and corresponding to the loss of the two CH_2Cl_2 guest molecules per formula (calculated 22.2%). In the temperature range of 260–550°C, **1** underwent complicated multiple weight loss steps, with the total weight loss corresponding to loss of three of the four L1 ligands (observed 40.9%, calculated 41.0%). Further weight loss was observed above 550°C; the final product is black and amorphous. The thermal decomposition behavior of **2** is quite different from that of compound **1**. The TGA data for **2** shows that the first weight loss (36.4%) occurs from 210 to 300°C, corresponding to the loss of two L2 ligands (calculated 36.5%). On further heating, another weight loss between 305 and 388°C was observed, corresponding to the loss of the third L2 ligand (observed 18.3%, calculated 18.2%). Further weight loss was observed when **2** was heated above 400°C and a black, amorphous product remained. As for compound **3**, about 1.0% weight loss was observed in the temperature range of 55–75°C, which corresponds to the loss of water solvent molecules (calculated 1.0%). A second weight loss of 34.8% occurred between 200 and 210°C, which agrees well with a calculated value of 34.4% for the loss of two 1,3-bis(4-pyridyl)propane ligands. This ligands loss is followed

by a 34.5% (calculated 34.4%) weight loss from 280 to 338°C, corresponding to the release of the rest of the 1,3-bis(4-pyridyl)propane ligands. Further weight loss was observed above 390°C, accompanied by the decomposition of the $Co(NCS)_2$ unit. A black amorphous residue remained.

Magnetic properties. The magnetic susceptibilities of polycrystalline powders of compounds **1–3** were measured from 2 to 300 K in an applied field of 5 kOe. The plots of the inverse magnetic susceptibility versus temperature for all compounds were found to be linear down to the lowest temperature measured. The data follow the Curie Law (44). The experimental effective magnetic moments (μ_{exp}) were 4.62 μ_B for **1**, 4.71 μ_B for **2**, and 4.68 μ_B for **3**, which are slightly lower than the theoretical value (4.80 μ_B) but nonetheless agree well with other experimentally observed effective magnetic moments for Co(II). These magnetic data clearly show that the Co(II) centers are not interacting with each other as hoped for, and can be treated as isolated magnetic centers.

CONCLUSIONS

This study demonstrates that the long conjugated rigid bidentate ligands 1,4-bis(3-pyridyl)-2,3-diaza-1,3-butadiene (L1) and 2,5-bis(3-pyridyl)-3,4-diaza-2,4-hexadiene (L2) are capable of coordinating transition metal centers through both of the terminal 3-pyridyl nitrogen donors, generating novel coordination polymers. Three new coordination polymers **1–3** were synthesized from reactions of L1, L2, and the flexible 1,3-bis(4-pyridyl)propane ligand with $Co(NCS)_2 \cdot xH_2O$. The Co(II) center in all three compounds resides in a $\{CoN_6\}$ six-coordinate environment. A comparison between **1** and **2** shows that varying the *R* group from H to $-CH_3$ on the $-CR{=}N{-}N{=}CR-$ spacer is, for the same solvent system and metal-to-ligand ratio (1:2), a decisive factor in determining the orientation of the nitrogen donors on terminal pyridyl groups, and, moreover, the topologies of the polymeric products. Comparing **1** to **3** demonstrates the role of the functionalized $-CH{=}N{-}N{=}CH-$ spacer in clathrating small polar organic guest molecules, such as CH_2Cl_2. We are currently extending these results by preparing new Schiff-base ligands similar to L1 and L2 with different *R* functional groups and with different orientations of the nitrogen donors on the pyridyl rings. We anticipate this approach to be useful for the construction of a variety of new coordination polymers with novel polymeric patterns.

ACKNOWLEDGMENTS

Financial support was provided by the Department of Defense through Grant N00014-97-1-0806 and by the National Science Foundation through Grant DMR:9873570. The authors also thank Dr. Richard D. Adams for the use of his single crystal X-ray diffractometer.

REFERENCES

1. P. J. Hagrman, D. Hagrman, and J. Zubieta, *Angew. Chem. Int. Ed.* **38,** 2638 (1999).
2. A. J. Blake, N. R. Champness, P. Hubberstey, W.-S. Li, M. A. Withersby, and M. Schröder, *Coord. Chem. Rev.* **183,** 117 (1999).
3. S. Batten and R. Robson, *Angew. Chem. Int. Ed.* **37,** 1460 (1998).
4. O. M. Yaghi, G. Li, and H. Li, *Nature* **378,** 703 (1995).
5. O. M. Yaghi and H. Li, *J. Am. Chem. Soc.* **117,** 10401 (1995).
6. O. M. Yaghi, H. Li, and T. L. Groy, *J. Am. Chem. Soc.* **118,** 9096 (1996).
7. M. Fujita, H. Oka, K. Yamaguchi, and K. Ogura, *Nature* **378,** 469 (1995).
8. M. Fujita, Y. J. Kwon, O. Sasaki, K. Yamaguchi, and K. Ogura, *J. Am. Chem. Soc.* **117,** 7287 (1995).
9. P. Losier and M. J. Zaworotko, *Angew. Chem. Int. Ed. Engl.* **35,** 2779 (1996).
10. K. N. Power, T. L. Hennigar, and M. J. Zaworotko, *Chem. Commun.* 595 (1998).
11. R. A. Heintz, H. Zhao, X. Ouyang, G. Grandinetti, J. Cowen, and K. R. Dunbar, *Inorg. Chem.* **38,** 144 (1999).
12. A. Mayr and J. Guo, *Inorg. Chem.* **38,** 921 (1999).
13. A. Mayr and L. F. Mao, *Inorg. Chem.* **37,** 5776 (1998).
14. L. F. Mao and A. Mayr, *Inorg. Chem.* **35,** 3183 (1996).
15. H. J. Choi and M. P. Suh, *J. Am. Chem. Soc.* **120,** 10622 (1998).
16. C. V. K. Sharma, G. A. Broker, J. G. Huddleston, J. W. Baldwin, R. M. Metzger, and R. D. Rogers, *J. Am. Chem. Soc.* **121,** 1137 (1999).
17. M. Fujita, Y. J. Kwon, S. Washizu, and K. Ogura, *J. Am. Chem. Soc.* **116,** 1151 (1994).
18. W. Lin, O. R. Evans, R.-G. Xiong, and Z. Wang, *J. Am. Chem. Soc.* **120,** 13272 (1998).
19. G. B. Garder, D. Venkataraman, J. S. Moore, and S. Lee, *Nature* **374,** 792 (1995).
20. G. B. Garder, Y.-H. Kiang, S. Lee, A. Asgaonkar, and D. Venkataraman, *J. Am. Chem. Soc.* **118,** 6946 (1996).
21. O. Kahn, Y. Pei, M. Verdguer, J. P. Renard, and J. Sletten, *J. Am. Chem. Soc.* **110,** 782 (1998).
22. K. Inoue, T. Hayamizu, H. Iwamura, D. Hashizume, and Y. Ohashi, *J. Am. Chem. Soc.* **118,** 1803 (1996).
23. H. Tamaki, Z. J. Zhong, N. Matsumoto, S. Kida, M. Koikawa, N. Achiwa, Y. Hashimoto, and H. Okawa, *J. Am. Chem. Soc.* **114,** 6974 (1992).
24. Y.-B. Dong, R. C. Layland, M. D. Smith, N. G. Pschirer, U. H. F. Bunz, and H.-C. zur Loye, *Inorg. Chem.* **38,** 3056 (1999).
25. Y.-B. Dong, R. C. Layland, M. D. Smith, N. G. Pschirer, U. H. F. Bunz, and H.-C. zur Loye, *Chem. Mater.* **11,** 1415 (1999).
26. Y.-B. Dong, M. D. Smith, R. C. Layland, and H.-C. zur Loye, *Inorg. Chem.* **38,** 5027 (1999).
27. Y.-B. Dong, M. D. Smith, R. C. Layland, and H.-C. zur Loye, *J. Chem. Soc. Dalton Trans.* 775 (2000).
28. Y.-B. Dong, M. D. Smith, R. C. Layland, and H.-C. zur Loye, *Chem. Mater.* **12,** 1156 (2000).
29. Y.-B. Dong, M. D. Smith, and H.-C. zur Loye, *Inorg. Chem.*, in press.
30. J.-M. Lehn, *Angew. Chem. Int. Ed. Engl.* **29,** 1304 (1990).
31. J.-M. Lehn, *Angew. Chem. Int. Ed. Engl.* **27,** 89 (1998).
32. "SHELXTL," Version 5.1. Bruker AXS, Inc., Madison, WI, 1997.
33. N. Walker and D. Stuart, *Acta Crystallogr. A* **39,** 158 (1996).
34. J. Lu, T. Paliwala, S. C. Lim, C. Yu, T. Niu, and A. J. Jacobson, *Inorg. Chem.* **36,** 923 (1997).
35. F. Lloret, G. D. Munno, M. Julve, J. Cano, R. Ruiz, and A. Caneschi, *Angew. Chem. Int. Ed.* **37,** 135 (1998).
36. The pore dimensions described here are crystallographic scalar quantities and do not account for the van der Waals radii of the atoms defining the pore.

37. R. W. Gable, B. F. Hoskins, and R. Robson, *J. Chem. Soc. Chem. Commun.* 1677 (1990).
38. R. Robson, B. F. Abrahms, S. R. Batten, R. W. Gable, B. F. Hoskins, and J. Liu, *in* "Supramolecular Architecture" (T. Bein, Ed.), Chap. 19, ACS Symposium Series 499. American Chemical Society, Washington, DC, 1992.
39. K. Biradha, K. V. Domasevitch, B. Moulton, C. Seward, and M. J. Zaworotko, *Chem. Commun.* 1327 (1999).
40. G. R. Desiraju, *Acc. Chem. Res.* **29,** 441 (1996).
41. O.-K. Jung, S. H. Park, K. M. Kim, and H. G. Jang, *Inorg. Chem.* **37,** 5781 (1998).
42. J. J. Novoa, M. C. Rovira, C. Rovira, J. Veciana, and J. Tarrés, *Adv. Mater.* **7,** 233 (1995).
43. M. L. Hernández, M. G. Barandika, M. K. Urtiaga, R. Cortés, L. Lezama, M. I. Arrioitua, and T. Rojo, *J. Chem. Soc. Dalton Trans.* 1401 (1999).
44. B. N. Figgis, "Introduction to Ligand Fields." Interscience, New York, 1966.